

Plasticity

CHAPTER PREVIEW

In this chapter, we are concerned with the deformation of ceramics leading to a permanent shape change. This is known as plastic deformation and is both nonrecoverable and irreversible. There are several mechanisms that are responsible for plastic deformation in crystalline materials: dislocation motion, vacancy motion, twinning, phase transformation. In metals at room temperature, dislocation motion is the most important of these mechanisms. In Chapter 12, we noted that dislocations don't move easily in ceramics, and that this is the reason for their inherent brittleness. Nevertheless, dislocation motion is observed in ceramics under specific loading conditions. In general, plastic deformation of ceramics requires high temperatures, and this is important because:

- We often process ceramics at high temperature.
- Many potential applications for ceramics, such as in fuel cells and engines, require them to be stable at high temperature.

We know that glass flows and that we can produce complex shape changes in glass. There are no dislocations in glass, so how does plastic deformation occur? The other question is: does the plastic deformation of glass always require a high temperature?

Selecting ceramics for use at high temperatures or under applied load requires consideration of their long-term stability. Time-dependent deformation is known as creep, and creep resistance is a critical design parameter. Even if creep doesn't lead to failure, a change in shape or size may render a component useless. The mechanism responsible for creep depends on temperature, stress, and the microstructure of the ceramic.

17.1 PLASTIC DEFORMATION

The onset and extent of plastic deformation is often measured when the $\sigma - \epsilon$ behavior of a material is being determined. We showed some general $\sigma - \epsilon$ curves in Chapter 16. In Figure 17.1, $\sigma - \epsilon$ curves obtained for crystals of KBr and MgO tested in bending are shown. From these curves we can identify several parameters that may already be familiar to you from discussion of the mechanical properties of metals.

Proportional limit P : corresponds to departure from linearity and is defined as the onset of plastic deformation. If the transition from elastic to plastic deformation is gradual, it may be difficult to determine precisely where P is, and sometimes it is better avoided.

Yield strength, σ_y : the stress determined by drawing a line parallel to the linear part of the $\sigma - \epsilon$ curve at some specified strain offset. We usually use a strain of 0.002. To compare the values of σ_y in Figure 17.1, you may

recall that for metals we see a wide range of values (e.g., for a low-strength aluminum alloy, $\sigma_y = 35$ MPa; for a high-strength steel, $\sigma_y > 1,400$ MPa). We usually say yield strength rather than yield stress. Strength is a material property; stress is a measure of the applied load.

Fracture strength, σ_F : the stress at fracture. Because ceramics are often tested in bending, we don't see any reduction in cross-sectional area during the test as we often do in a tensile test with a metal. As a result, we would not expect to see a maximum in the $\sigma - \epsilon$ curve corresponding to the tensile strength or ultimate tensile strength.

Figure 17.2 shows a $\sigma - \epsilon$ curve for LiF that illustrates an abrupt elastic-plastic transition. Plastic deformation begins at the upper yield point, and there is a decrease in stress. At the lower yield point, deformation continues at a lower stress level. This type of behavior is similar to that of some low-carbon steels and also aluminum oxide and magnesium oxide at high temperatures.

17.2 DISLOCATION GLIDE

Dislocation glide (or slip) is a primary mechanism for plastic deformation in crystals. Slip takes place discontinuously in bands, as illustrated in Figure 17.3. Although we often think of dislocations in ceramics as immobile, they can glide, as shown in Figure 17.4A. In this case, a crystal of LiF has been plastically bent, and the dislocations are revealed by etching. Figure 17.4B is a dark-field transmission electron microscopy (TEM) image that shows a glide band in spinel. The dislocations are visible in the dark-field image as the bright lines against a dark background.

Both the direction of slip and usually the slip plane have a definite crystallographic orientation; together they are known as the slip system. Slip systems for several ceramics are given in Table 17.1. Primary slip systems are those for which slip is easiest; it is more difficult on secondary slip systems and is usually activated at higher temperature. What determines the slip system for ceramics?

The slip direction is usually that having the smallest spacing between atoms or ions of the same type (highest linear density). In metals, the slip plane is often the closest packed plane (highest planar density). In ceramics, we

consider planar density, but there is often the additional consideration of electrostatic interaction between ions. We can illustrate these considerations by

looking at the familiar rock salt structure (structure of NaCl and MgO). This is an interesting example to start with because the first studies of crystal plasticity, which were conducted by Reusch in 1867, were conducted using sodium chloride. He concluded that the slip system for NaCl is $\{110\}\langle 1\bar{1}0\rangle$.

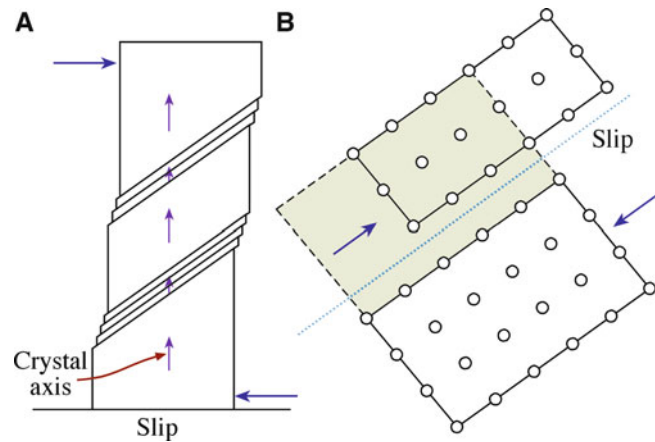


FIGURE 17.3. Slip bands. (A) Macroscopic appearance. (B) Atomic movements.

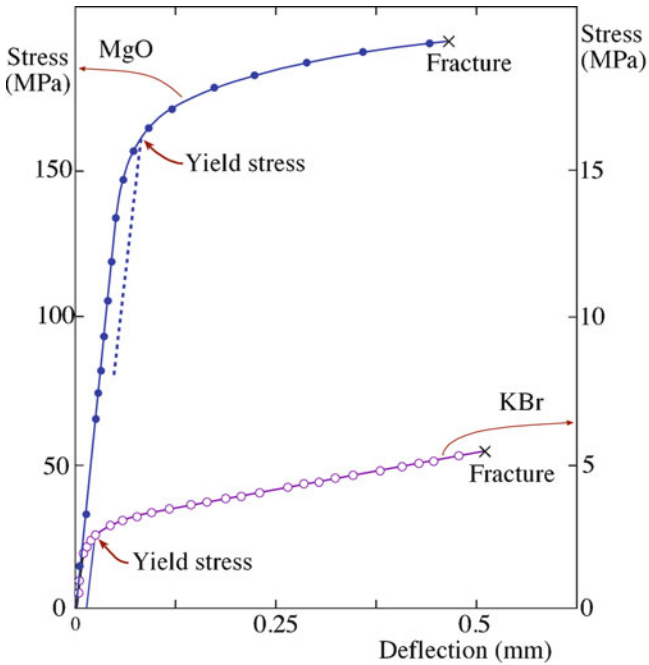


FIGURE 17.1. Stress–strain curves for KBr and MgO crystals tested in bending.

SLIP SYSTEM

A plane and a direction and is represented as $\{hkl\}\langle uvw\rangle$.

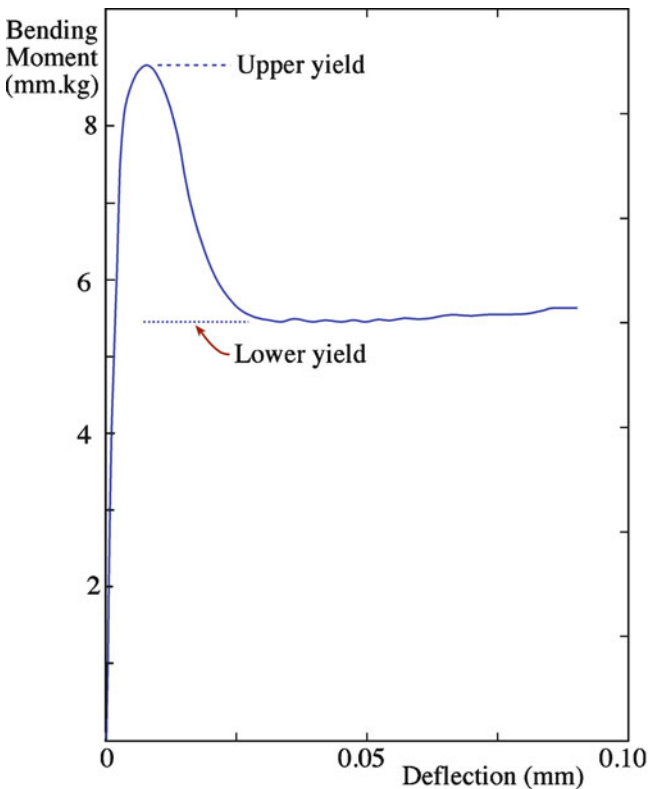


FIGURE 17.2. Stress–strain curve for a LiF single crystal.

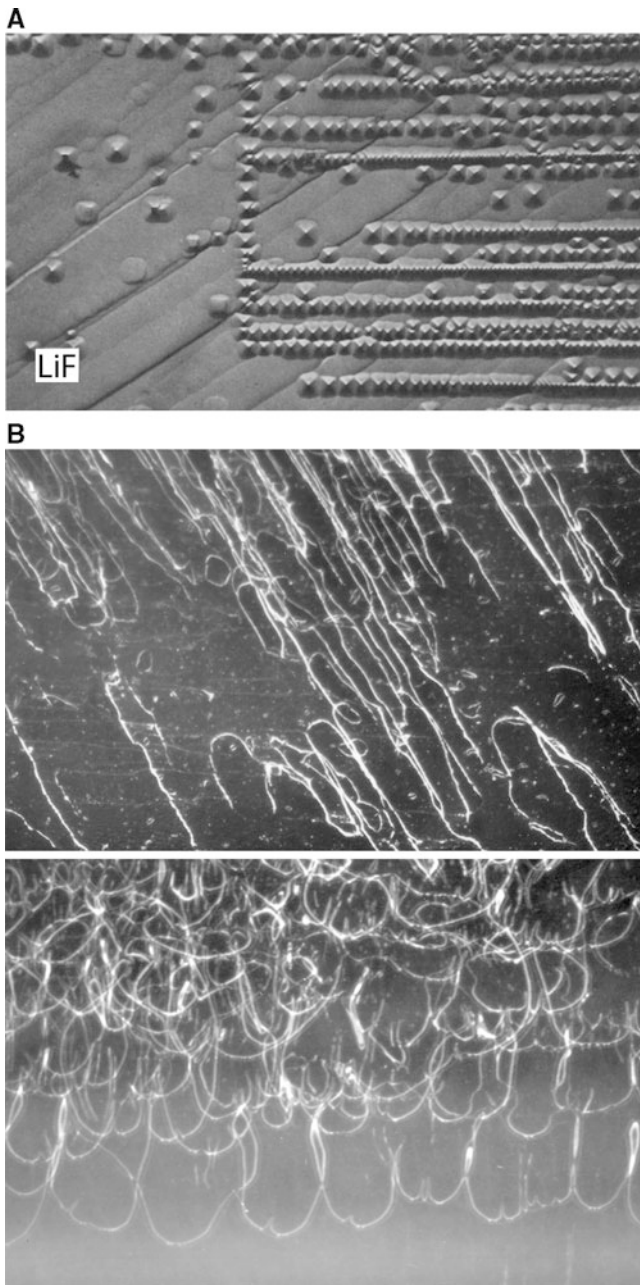


FIGURE 17.4. (A) Glide bands in LiF revealed by etching. (B) “Glide” bands in spinel: (top) 200°C; (bottom) 950°C.

The choice of slip plane has often been explained by considering the position of ions during slip. Figure 17.5 compares the ion positions during slip on {100} and {110}. The key difference is that slip on {100} would increase the distance between opposite ions, whereas during slip on {110} oppositely charged ions are brought closer together. The overall effect is that slip on {110} would lead to a decrease in electrostatic interaction energy. Clearly, this is not the complete story, as we mentioned in Section 12.5. Not all crystals with the rock salt structure share the same

slip system as shown in Table 17.2. The primary glide plane depends on the atoms present. For PbS and PbTe, the primary glide plane is {100}, not {110}. The explanation proposed back in 1930 by Buerger is based on the polarizability or “deformability” of the ions. As the sum of the polarizability of both ions increases, there is increasing ease of slip on {100} and increasing plasticity.

17.3 SLIP IN ALUMINA

The slip system for α -alumina (corundum) is given in Table 17.1. The primary slip plane is the basal plane, (0001); the slip direction is $\langle 11\bar{2}0 \rangle$. The arrangement of atoms on the slip plane is shown in Figure 12.13A. For the oxygen ions, the close-packed direction is actually $\langle 1100 \rangle$; this is not the slip direction because we need to consider what happens to the aluminum ions, which occupy only two thirds of the octahedral interstices. Slip along $\langle 11\bar{2}0 \rangle$ preserves the stacking sequence of the aluminum ions. Temperatures around 1,300°C are needed before significant plastic deformation is observed in single-crystal alumina. At even higher temperatures, other slip systems become activated, as summarized in Table 17.3.

Because of the large Burgers vector involved, the combined motion of partial dislocations may lead to slip. You can remember the background to this argument from Chapter 12. Graphite is another hexagonal ceramic where slip has been found to occur by the motion of partial dislocations.

17.4 PLASTIC DEFORMATION IN SINGLE CRYSTALS

There are many mechanisms that can lead to plastic deformation in single crystals, but the most important is slip. The two things that we need to consider are the inherent resistance to the movement of dislocations provided by the periodicity of the lattice and the orientation of the crystal with respect to the applied stress.

Lattice Resistance: the stress, τ_f , needed to move a dislocation along the slip plane is known as the Peirels-Nabarro (or frictional stress) and is given by c :

$$\tau_f = \mu \exp\left(-\frac{2\pi w}{b}\right) \quad (17.1)$$

The stress is clearly a function of the crystal structure and bonding, it depends on b and w . You may recall from Chapter 12 that dislocation widths in covalent solids are quite narrow ($w \sim b$) compared with those in face-centered cubic (fcc) metals ($w \sim 10b$).

- For metals $\tau_f \sim 10 \text{ MPa} \sim 10^{-4} \mu$, these stresses are fairly small, and dislocations can move freely. The yield stress is determined primarily by interactions

TABLE 17.1 Slip Systems for Several Ceramics

Material	Crystal structure	Slip systems		Activation temperature (°C)	
		Primary	Secondary	Primary	Secondary
Al ₂ O ₃	Hexagonal	{0001}<1120>	Several	1,200	
BeO	Hexagonal	{0001} <1120>	Several	1,000	
MgO	Cubic (NaCl)	{110} <110>	{001} <110>	0	1,700
MgO·Al ₂ O ₃	Cubic (spinel)	{111}<110>	{110}<110>	1,650	
β-SiC	Cubic (ZnS)	{111}<110>		>2,000	
β-Si ₃ N ₄	Hexagonal	{1010}<0001>		>1,800	
TiC, (ZrC, HfC, etc.)	Cubic (NaCl)	{111}<110>	{110}<110>	900	
UO ₂ , (ThO ₂)	Cubic (CaF ₂)	{001}<110>	{110}<110>	700	1,200
ZrB ₂ , (TiB ₂)	Hexagonal	{0001}<1120>		2,100	
C (diamond)	Cubic	{111}<110>			
C (graphite)	Hexagonal	{0001}<1120>			
β-SiO ₂	Hexagonal	{0001}<1120>			
CaF ₂ , (BaF ₂ , etc.)	Cubic	{001}<110>			
CsBr	Cubic (CsCl)	{110}<001>			
TiO ₂	Tetragonal	{110}<110>	{110}<001>		
WC	Hexagonal	{1010}<0001>	{1010}<1120>		

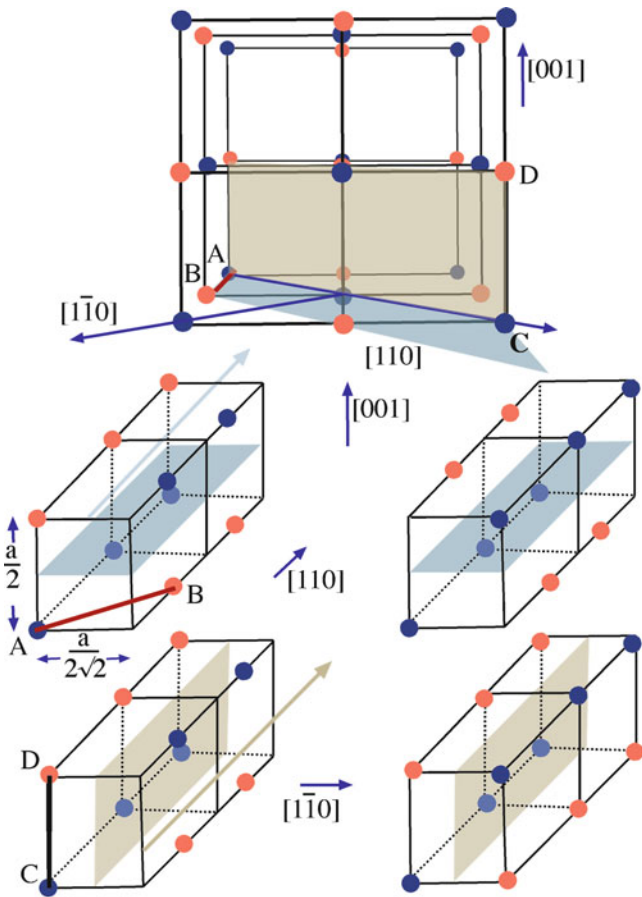


FIGURE 17.5. Comparison of slip in the rock salt structure on {100} and {110} planes.

between dislocations and other defects, such as impurities.

- For simple ionic ceramics (e.g., NaCl and CaF₂) $\tau_f \sim 10\text{--}100 \text{ MPa} \sim 10^{-4} \mu \text{ to } 10^{-3} \mu$.

- For complex ionic ceramics (e.g., Al₂O₃) and covalent ceramics (e.g., SiC), $\tau_f \sim 1,000 \text{ MPa} \sim 10^{-2} \mu$. Dislocations have low mobility, and lattice resistance is the main obstacle.

Orientation: plastic deformation depends not only on how easy it is for the dislocations to glide on their slip plane but also the orientation of the slip plane and the slip direction with the applied stress. If we consider a single crystal subject to uniaxial tension, as illustrated in Figure 17.6, the shear stress acting on the slip plane in the slip direction is:

$$\tau_r = \sigma \cos\phi \cos\psi \tag{17.2}$$

where τ_r is the resolved shear stress.

For some structures it is possible to orient the crystal so that τ_r on all operative slip systems is zero. If this is the case, dislocation motion does not occur, and the crystal does not plastically deform at stresses below the theoretical lattice strength. For example, in MgO τ_r is zero when σ is applied along <111>. Under these loading conditions at elevated temperatures (>300°C), slip may occur on the secondary slip system: {001}<110>.

The critical resolved shear stress, τ_{crss} , is the minimum shear stress required to initiate slip for a particular slip system defined when $\sigma = \sigma_y$.

$$\tau_{crss} = \sigma_y (\cos\phi \cos\psi) \tag{17.3}$$

Figure 17.7A shows the stress–strain behavior for a single crystal that is favorably oriented for plastic flow.

TABLE 17.2 Comparison of Primary Glide Planes in Crystals Having the Rock Salt Structure

Crystal	Primary glide plane	Polarizability (10^{-30} m^{-3})			Lattice constant (nm)
		Anion	Cation	Total	
LiF	{110}	0.03	1.0	1.03	0.401
MgO	{110}	0.09	3.1	3.19	0.420
NaCl	{110}	0.18	3.7	3.88	0.563
PbS	{100}	3.1	10.2	13.3	0.597
PbTe	{100}	3.1	14.0	17.1	0.634

TABLE 17.3 Slip Systems in α -Alumina (Corundum)

System name	Slip system	Remarks
Basal	(0001) $1/3\langle 2\bar{1}\bar{1}0 \rangle$	Dominant system under shear superimposed on 1 atm of pressure
Prismatic	$\{1\bar{2}10\}\langle 10\bar{1}0 \rangle$ $\{1\bar{2}10\}\langle 10\bar{1}1 \rangle$	Occurs above 1,600°C under shear superimposed on 1 atm of pressure
Pyramidal	$\{1\bar{1}02\}\langle 01\bar{1}1 \rangle$ $\{10\bar{1}1\}\langle 01\bar{1}1 \rangle$	Occurs above 1,600°C under shear superimposed on 1 atm of pressure

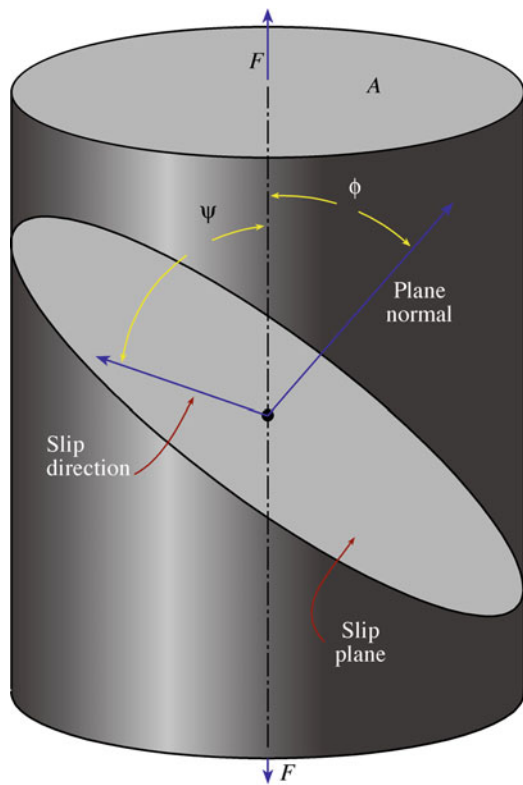


FIGURE 17.6. Geometry used to determine the critical resolved shear stress.

This type of behavior is seen in MgO and other ceramics with the rock salt structure. There are three distinct stages.

- Stage I: easy glide of dislocations with the possibility of large strains (~20%)
- Stage II: interaction of dislocations on intersecting slip planes, resulting in work hardening
- Stage III: cross-slip

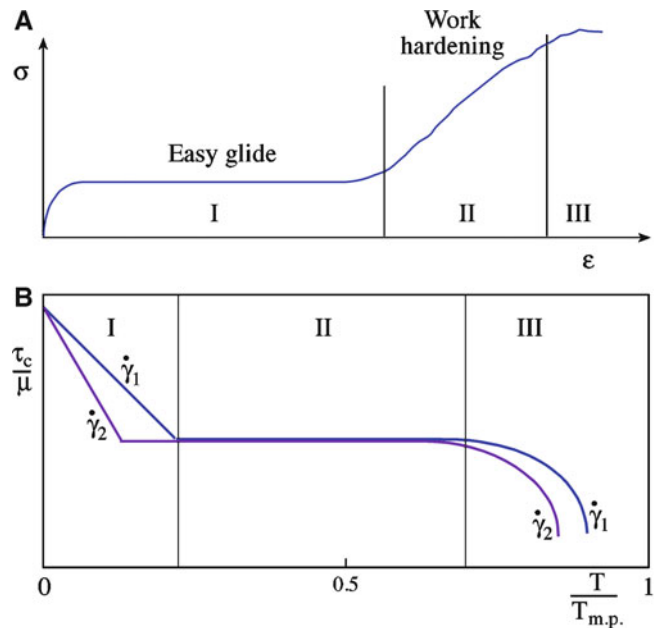


FIGURE 17.7. (A) Stress–strain curve for a crystal suitably oriented for plastic flow. (B) Temperature dependence of the normalized critical resolved shear stress for two strain rates, where $\dot{\gamma}_1 > \dot{\gamma}_2$.

The value of τ_{crss} depends on test conditions, such as temperature and strain rate, as shown in Figure 17.7B. We can again identify three distinct behaviors.

- Region I: τ_{crss} decreases with increasing temperature and decreasing strain rate. Thermal fluctuations enhance dislocation motion.
- Region II: τ_{crss} is independent of temperature and strain rate. There is interaction between dislocations and between dislocations and other defects.
- Region III: τ_{crss} again decreases with increasing temperature and decreasing strain rate. At high temperatures diffusion processes can become important.

17.5 PLASTIC DEFORMATION IN POLYCRYSTALS

Plastic deformation is more difficult in polycrystals than in single crystals because now we have to consider what happens at the grain boundaries. Grain boundaries act as barriers to dislocation motion; and if adjacent grains are not favorably oriented for slip to continue, dislocations pile up at the boundary.

A polycrystal needs five independent slip systems before it can undergo an arbitrary strain. This requirement is known as the von Mises criterion. A slip system is independent if the same strain cannot be produced from a combination of slip on other systems. From Table 17.4 you can see why MgO might be ductile when stressed as a single crystal, whereas in polycrystalline form it is brittle except at high temperature where secondary slip systems operate. For polycrystalline MgO, the brittle-to-ductile transition occurs at $\sim 1,700^\circ\text{C}$, as shown in Figure 17.8. Some cubic materials (e.g., TiC, MgAl_2O_4) do have enough independent slip systems; but the Peierls-Nabarro stress is high, making dislocations immobile except at high temperature.

The Hall–Petch relation (equation 14.9) tells us the effect of grain size, d , on the stress required to make the dislocation move in a polycrystalline sample. The origin of the relation is that the stress to operate a Frank-Read source increases as the size of the source decreases. If the grain size decreases, then the maximum size of the Frank-Read source also decreases. The result is the famous $d^{1/2}$ relationship.

Hence, the grain size of a polycrystalline ceramic is important in determining the yield strength and the fracture strength of ceramics. Figure 17.9 illustrates the background to equation 14.9. Slip starts in the most favorably oriented grains. If the material is to plastically

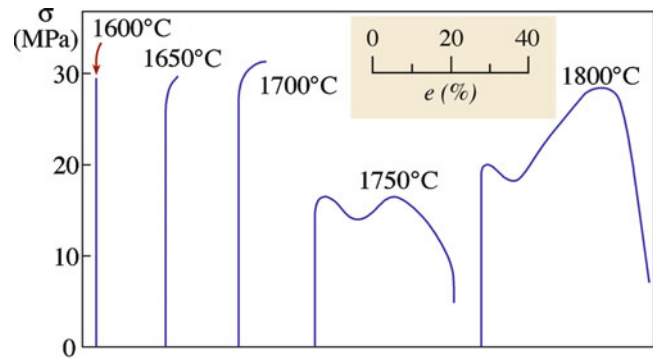


FIGURE 17.8. Stress–strain curves for polycrystalline MgO as a function of temperature.

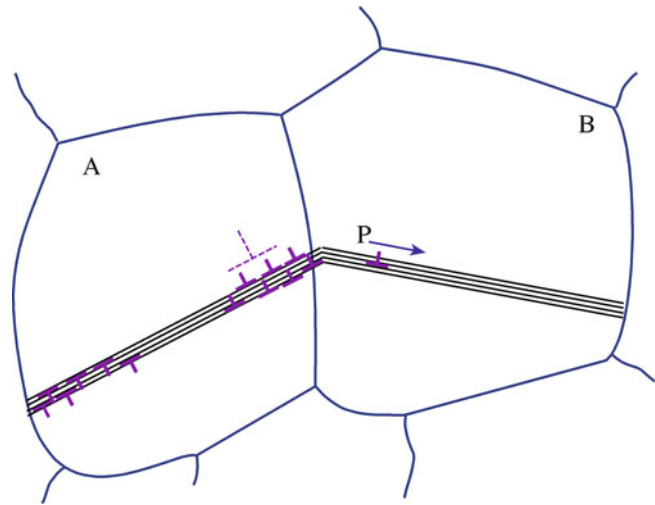


FIGURE 17.9. Slip propagation from grain A to grain B.

TABLE 17.4 Independent Slip Systems for Some Ceramics

Lattice type	Crystal	Slip system	No. of independent systems
Rock salt	MgO, NaCl, LiF, NaF	$\{110\}\langle 1\bar{1}0\rangle$	2
Rock salt	MgO, NaCl, LiF, NaF	$\{110\}\langle 1\bar{1}0\rangle$ $\{001\}\langle 1\bar{1}0\rangle$ $\{111\}\langle 1\bar{1}0\rangle$	5 at high temperature
Fluorite	UO_2 and CaF_2	$\{001\}\langle 1\bar{1}0\rangle$	3
	TiC and UC	$\{111\}\langle 1\bar{1}0\rangle$	5
Spinel	MgAl_2O_4	$\{111\}\langle 1\bar{1}0\rangle$	5
Fluorite	UO_2 and CaF_2	$\{110\}\langle 1\bar{1}0\rangle$ $\{001\}\langle 1\bar{1}0\rangle$ $\{110\}\langle 1\bar{1}0\rangle$ $\{111\}\langle 1\bar{1}0\rangle$	5 at high temperatures
Hexagonal	Al_2O_3 , C (graphite), BeO	$\{0001\}\langle 11\bar{2}0\rangle$	2
Hexagonal	Al_2O_3 , C (graphite), BeO	$\{0001\}\langle 11\bar{2}0\rangle$ $\{1\bar{2}10\}\langle 10\bar{1}0\rangle$ $\{1\bar{2}10\}\langle 10\bar{1}1\rangle$ $\{1\bar{1}02\}\langle 01\bar{1}1\rangle$ $\{10\bar{1}1\}\langle 01\bar{1}1\rangle$	5 at high temperatures
Sphalerite	ZnS, β -SiC	$\{111\}\langle 1\bar{1}0\rangle$	5

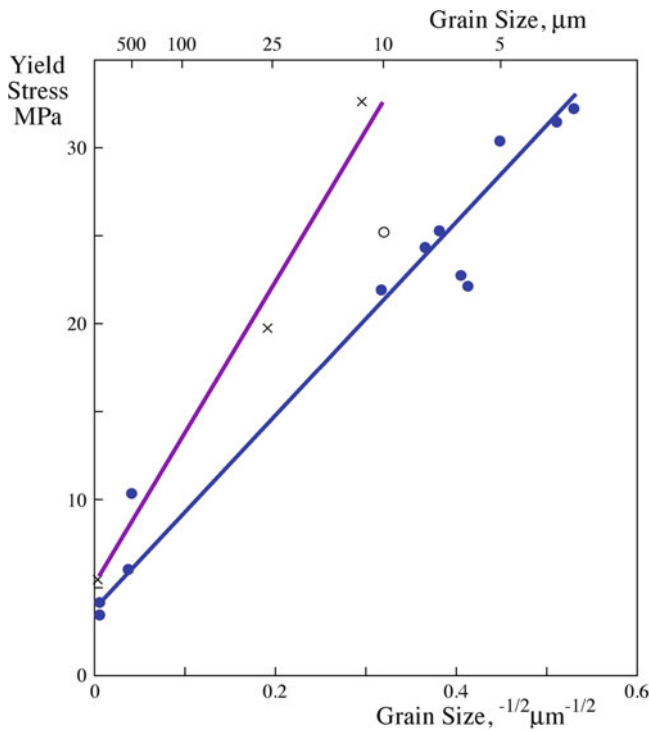


FIGURE 17.10. Grain size dependence of yield strength for KCl. Filled circles: pure material with a $\langle 100 \rangle$ texture; open circles: pure material with $\langle 111 \rangle$ texture; crosses: Sr-doped KCl.

deform, then slip must propagate from one grain to the next. Stress concentrations are built up at the grain boundary at P, and they are greater when the length of the slip band, or the grain size, is large. For deformation to continue, the stress must be sufficient to start dislocation motion in an adjacent grain; and this is easier for large-grain samples. The increase in strength of polycrystalline KCl as the grain size decreases (an illustration of the Hall–Petch phenomenon) is shown in Figure 17.10.

In some cases, the Hall–Petch equation appears to hold when the grain size is on the order of several nanometers. In these cases, deformation cannot be due to dislocation glide, and perhaps equation 14.9 is best thought of as a scaling law. Figure 17.11 shows a Hall–Petch plot for TiO_2 over a wide range of grain sizes. At the very smallest grain sizes studied, the behavior is inverse or negative Hall–Petch. The reasons for this transition are not well understood, and the transition does not appear to occur for all nanomaterials.

17.6 DISLOCATION VELOCITY AND PINNING

Figure 17.12 shows the stress dependence of dislocation velocity for CaF_2 . At low stresses, the relationship has the form:

$$v = \left(\frac{\tau}{\tau_0} \right)^p \quad (17.4)$$

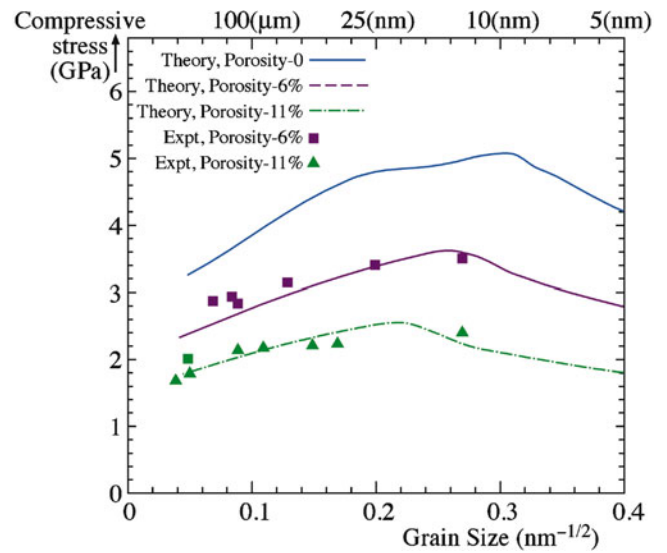


FIGURE 17.11. Compressive yield stress as a function of grain size for nanocrystalline TiO_2 at three levels of porosity.

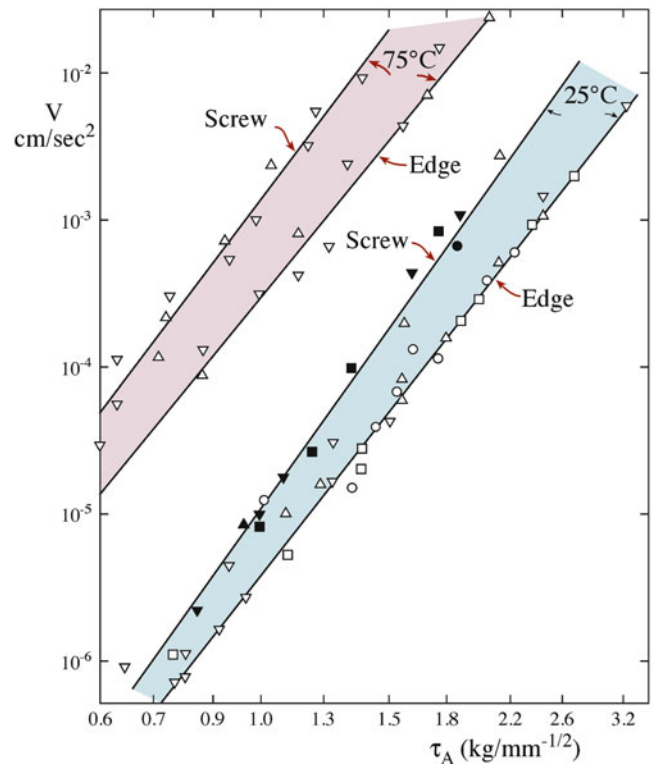


FIGURE 17.12. Stress dependence of dislocation velocity.

Both τ_0 and p are material constants: τ_0 is the shear stress for unit dislocation velocity, and p is the velocity stress exponent that describes the stress dependence of the dislocation velocity. Values are given for some materials in Table 17.5. At very high stresses, equation 17.4 does not hold as the maximum dislocation velocity in a crystal

TABLE 17.5 Values of the Constants in Equation 17.4 for Some Materials^a

Material	τ_o (MPa)	ρ
Zn	0.03	1
Cu	0.03	1
Mo	64.8	7
Nb	48.3	16
Fe + 3%Si	193.1	30
NaCl	1.45	8
LiF	11.7	25
Ge (440°C)	965 GPa	1

^aAt room temperature, except for Ge

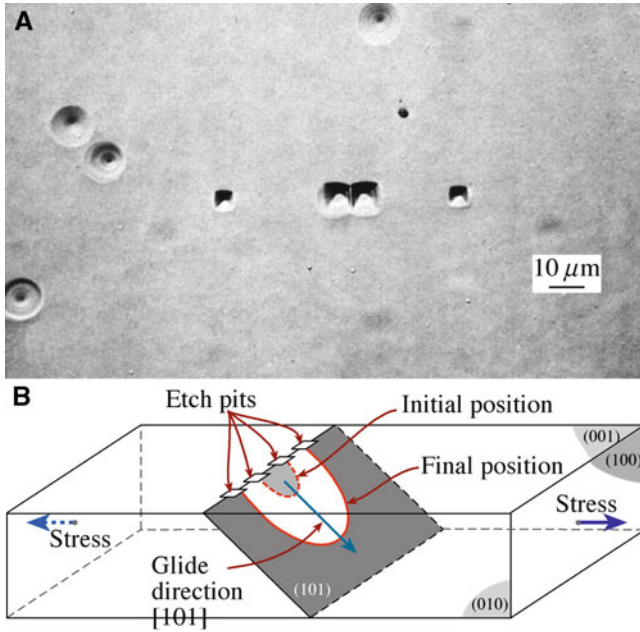


FIGURE 17.13. Etch pits show the motion of a dislocation loop in single crystal LiF.

equals the velocity of sound. Determination of dislocation velocity has been done using the etch-pit technique, as illustrated in Figure 17.13 for LiF.

Dislocations in ceramics can be pinned by solute atoms just as they can in metals, as shown in Figure 17.14. The dislocations are impeded because of their interaction with the stress field around the impurity. This effect has long been used to strengthen metals.

17.7 CREEP

Creep is time-dependent permanent deformation that is often due to diffusion processes rather than dislocation motion. Engineers need to consider creep in cases where ceramic components are used in load-bearing applications at high temperature. It is necessary to specify a particular

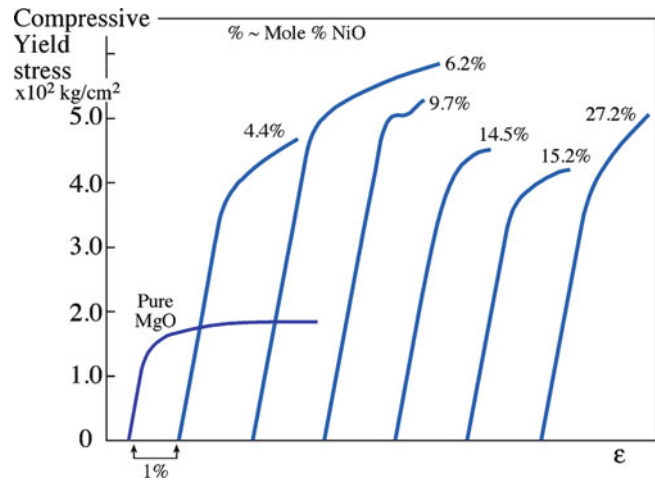


FIGURE 17.14. Solute hardening in MgO.

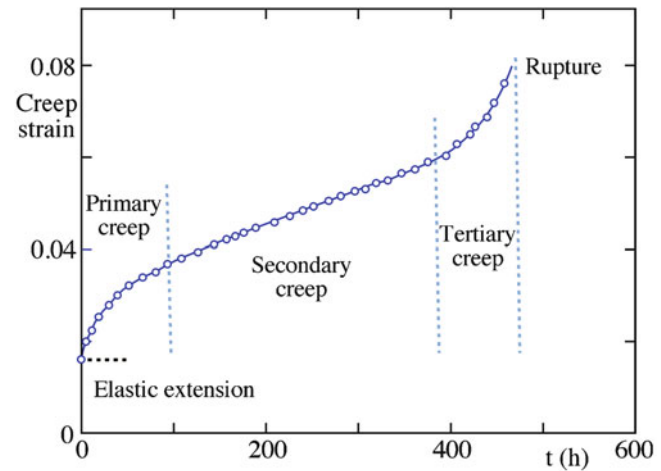


FIGURE 17.15. Creep curve illustrating three distinct regimes.

maximum strain that is acceptable during the anticipated lifetime of the component.

In general, creep behavior of ceramics is similar to that of metals. However, in ceramics it usually occurs at higher temperatures, typically $>0.5T_m$. In comparison, creep is a consideration in aluminum alloys at 100°C and in polymers at room temperature. Creep is particularly important in ice, which creeps extensively at low temperatures. The creep of ice is responsible for the movement of glaciers and the spreading of the Antarctic ice cap.

Figure 17.15 shows a general creep curve. There are three regimes.

- Transient or primary creep: following spontaneous elastic strain, the creep rate (also referred to as creep strain rate) decreases with time from an initially high value. This stage of creep is often represented by an equation of the form:

$$\epsilon = \beta T^m \quad (17.5)$$

where β is a constant, and M varies from 0.03 to 1.0 depending on the material, stress, and temperature. In some ceramics (e.g., SiC fibers) this may be the only stage shown.

- Steady-state or secondary creep: strain increases linearly with time, the creep rate is constant, and deformation may continue for a long time. This is the most important regime. The equation for secondary creep is:

$$\epsilon = Kt \quad (17.6)$$

where K is a constant that depends on stress and temperature. The mechanisms for this stage are discussed in the next sections.

- Tertiary creep: a rapid increase in creep rate just before failure. This stage is often missing for ceramics.

The creep behavior of a ceramic is determined by measuring the strain rate as a function of load. In the simplest approach, a load is attached to the sample, which is heated; the deformation is then measured as a function of time. Because of the problems we mentioned earlier of performing tensile tests on ceramics, the load is usually applied by bending. The disadvantage of bending tests is the inhomogeneous stress state, which changes during creep deformation. The creep behavior of ceramics is different if the load is applied in tension or compression; and compressive creep tests may, although rarely, be performed.

STRAIN & CREEP

Elastic strain: $\epsilon_0 = \sigma/\mathcal{E}$

Creep rate: $\dot{\epsilon}_c = \frac{d\epsilon_c}{dt}$

ϵ_c is the creep strain

There are three mechanisms for creep, and we describe each of them in the following sections.

17.8 DISLOCATION CREEP

Dislocation creep occurs by dislocation motion (i.e., glide and climb). For the climb-controlled process, the creep rate can be expressed as:

$$\dot{\epsilon} = \frac{\alpha D_L \mu b}{kT} \left(\frac{\sigma}{\mu} \right)^n \quad (17.7)$$

which we can simplify by taking all of the “constants” into a temperature-dependant constant Γ .

$$\dot{\epsilon} = \Gamma \sigma^n \quad (17.8)$$

This is a simple power law equation; and when $n > 1$, we refer to it as power law creep. For climb, n is in the range of 4–5; for a glide-controlled process, $n = 3$.

17.9 DIFFUSION-CONTROLLED CREEP

Diffusion-controlled creep is due to atomic diffusion. There is no dislocation motion. Considering the single crystal shown in Figure 17.16, Nabarro (1948) showed that vacancies would move from the faces under tension to those under compression. There is a counterflow of atoms, and we get a permanent shape change as a result.

TERMS IN CREEP EQUATIONS

α	A constant
D_L	Lattice diffusivity
k	Boltzmann's constant
b	Burgers vector
T	Absolute temperature
σ	Applied stress
μ	Shear modulus
m	Grain size exponent
n	Stress exponent
Ω	Atomic volume
d	Grain size
D_{gb}	Grain boundary diffusivity
δ	Grain boundary width
A	Dimensionless constant
D	Diffusion coefficient

For Nabarro-Herring creep, the creep rate is given by:

$$\dot{\epsilon} = \frac{\alpha D_L \sigma \Omega}{d^2 kT} \quad (17.9)$$

In this case, the constant, α , depends on the extent of grain-boundary sliding, as determined by Herring (1950).

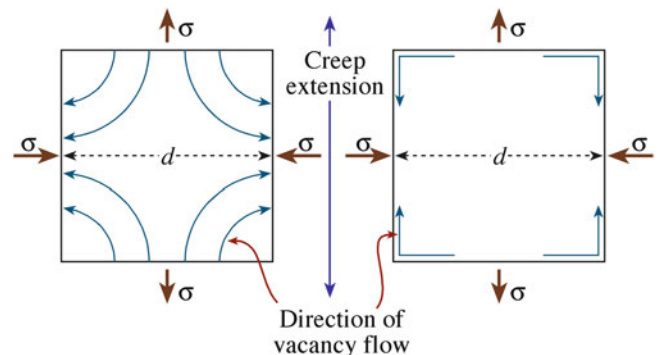


FIGURE 17.16. Nabarro-Herring creep.

For simple tension test measurements under steady-state conditions, $\alpha = 13.3$.

We assume that:

- The main source and sink for vacancies are grain boundaries.
- We have equilibrium.
- There is no cavitation.

The important points about Nabarro-Herring creep are:

- Temperature has to be high enough to allow significant vacancy diffusion.
- Diffusion is considered to occur through the bulk of the material.
- Because of the d^{-2} dependence, the creep rate increases with decreasing grain size (shorter diffusion distance).
- The creep rate is proportional to the applied stress (at least for lower stresses).
- There is linear dependence between the strain rate and stress.

At lower temperatures and for fine-grained ceramics, grain boundary diffusion may be the dominant path. In these situations, the process is termed Coble creep (Coble 1963); and the creep rate is:

$$\dot{\epsilon} = \frac{150\Omega\delta D_{gb}\sigma}{\pi d^3 kT} \quad (17.10)$$

The important points to note from equation 17.10 are:

- Creep rate varies as d^{-3} —hence it is important for very fine-grained ceramics.
- $D_{gb} > D_L$, so Coble creep is favored at lower temperatures.

Nabarro-Herring and Coble creep can take place in parallel, so that the creep rates involve both components and both diffusion coefficients. In ceramics, we also have the situation where both anions and cations are diffusing, adding further complications to the creep rate equations. If there is a large difference in the diffusion rates, then the creep rate is controlled by the slower diffusing species along the faster diffusing path.

17.10 GRAIN-BOUNDARY SLIDING

In some ceramics, an intergranular film (IGF) forms during fabrication, often due to the addition of a sintering aid. If this phase softens at high temperature, then we get creep by grain boundary sliding. The glass viscosity, η , which is a function of temperature, controls the creep rate. As the temperature increases, the viscosity decreases, which is usually represented by an empirical relation known as the

Vogel-Fulcher-Tammann (VFT) equation or sometimes simply the Fulcher equation.

$$\ln \eta = A + \frac{B}{T - T_0} \quad (17.11)$$

A , B , and T_0 are constants for a particular glass. The VFT equation works very well except at temperatures close to the glass transition temperature, T_g .

There are several mechanisms that can result in a permanent change in shape. In one mechanism, the glass is squeezed out of the boundaries during compression flowing to those under tension. Proof of this mechanism comes from high-resolution TEM, which can be used to measure directly the thickness, w , of the IGF. In these cases:

$$\dot{\epsilon} = \frac{\alpha w^3 \sigma}{\eta_0 d^3} \quad (17.12)$$

Another proposed mechanism is that of dissolution and precipitation, which is illustrated in Figure 17.17. Here, grains dissolve in the liquid at points of high stress, and this solute then diffuses through the liquid and precipitates at regions of low stress. In this case the creep rate is:

$$\dot{\epsilon} = \frac{\alpha w \sigma \Omega^{\frac{2}{3}}}{\eta_0 d^3} \quad (17.13)$$

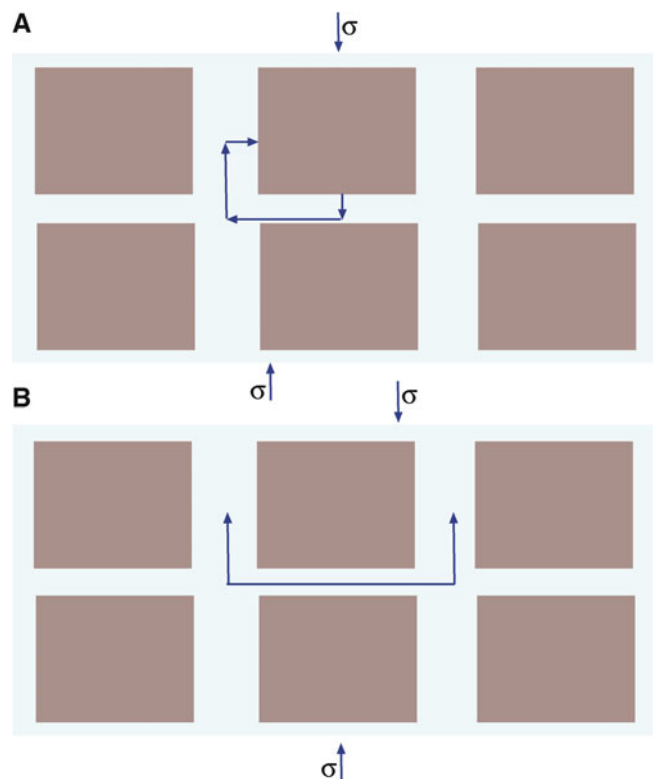


FIGURE 17.17. Dissolution-precipitation mechanism that could be operative in ceramics containing a glassy phase at the grain boundary.

This latter mechanism is similar to what happens during liquid-phase sintering (see Chapter 24). The requirements are that:

- The solid must have a certain amount of solubility in the liquid.
- The liquid must wet the solid.

The composition of the IGF is important in determining overall creep behavior. For example, using Y_2O_3 as a sintering aid for silicon nitride ceramics has been found to be superior to using MgO. Other important aspects of the microstructure are the grain size and the volume fraction of liquid present.

17.11 TERTIARY CREEP AND CAVITATION

Tertiary creep represents the final stage of creep deformation and involves an acceleration of the creep rate followed by failure of the component. This stage does not occur in all ceramics; and as we noted already, certain ceramics exhibit only primary creep. Tertiary creep involves the formation of cavities that lead to crack formation, often along grain boundaries. The cracks can propagate rapidly particularly under tensile loading.

Although the nucleation of cavities does not seem to be well understood at present, it is clear that cavitation depends on the microstructure. Porosity and second-phase particles, which are sources of stress concentration (see Chapter 18), can act as nucleation sites for cavitation and subsequent crack growth. Remember that pores can be found in most ceramics; even “pore-free” materials such as hot-pressed alumina may contain small pores. Cavitation occurs also in ceramics with IGFs. Nucleation of the cavities usually occurs at regions where the IGF is not homogeneous (e.g., nonwetted regions, gas bubbles, impurity particles).

Figure 17.18 shows cavity size distribution data for two polycrystalline aluminas. One is Lucalox (there is no glassy phase), and the other is 99% pure alumina with a glassy phase. The data were obtained using small-angle neutron scattering. For Lucalox, the number of pores increase with increasing creep strain, but their size does not increase—nucleation is the dominant process. For the alumina with a glassy phase, both the number and size of the pores increase with creep strain—we are getting both nucleation and growth.

17.12 CREEP DEFORMATION MAPS

From the previous sections you can see that there are a large number of creep mechanisms. They can be expressed by one general equation.

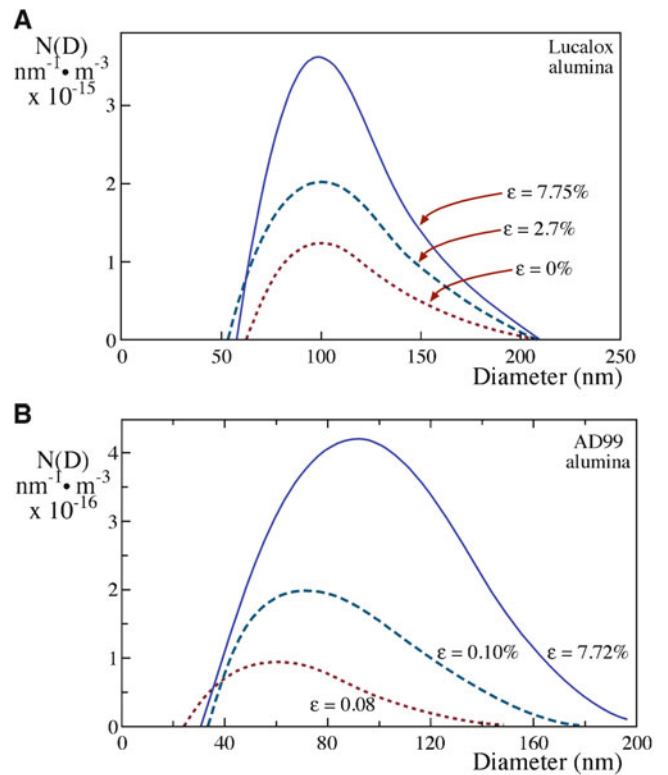


FIGURE 17.18. (A) Cavity-size distribution as a function of creep strain in alumina without a glassy phase (Lucalox). (B) Cavity-size distribution as a function of creep strain in alumina with a glassy phase (AD99).

TABLE 17.6 Creep Equation Exponents and Diffusion Paths for Various Creep Mechanisms

Creep mechanism	m	n	Diffusion path
<i>Dislocation creep mechanism</i>			
Dislocation glide climb, climb controlled	0	4–5	Lattice
Dislocation glide climb, glide controlled	0	3	Lattice
Dissolution of dislocation loops	0	4	Lattice
Dislocation climb without glide	0	3	Lattice
Dislocation climb by pipe diffusion	0	5	Dislocation core
<i>Diffusional creep mechanisms</i>			
Vacancy flow through grains	2	1	Lattice
Vacancy flow along grain boundaries	3	1	Grain boundary
Interface reaction control	1	2	Lattice/grain boundary
<i>Grain boundary sliding mechanisms</i>			
Sliding with liquid	3	1	Liquid
Sliding without liquid (diffusion control)	2–3	1	Lattice/grain boundary

$$\dot{\epsilon} = \frac{AD\mu b}{kT} \left(\frac{b}{d}\right)^m \left(\frac{\sigma}{\mu}\right)^n \quad (17.14)$$

The various creep mechanisms give rise to different values of the exponents, m and n , as shown in Table 17.6.

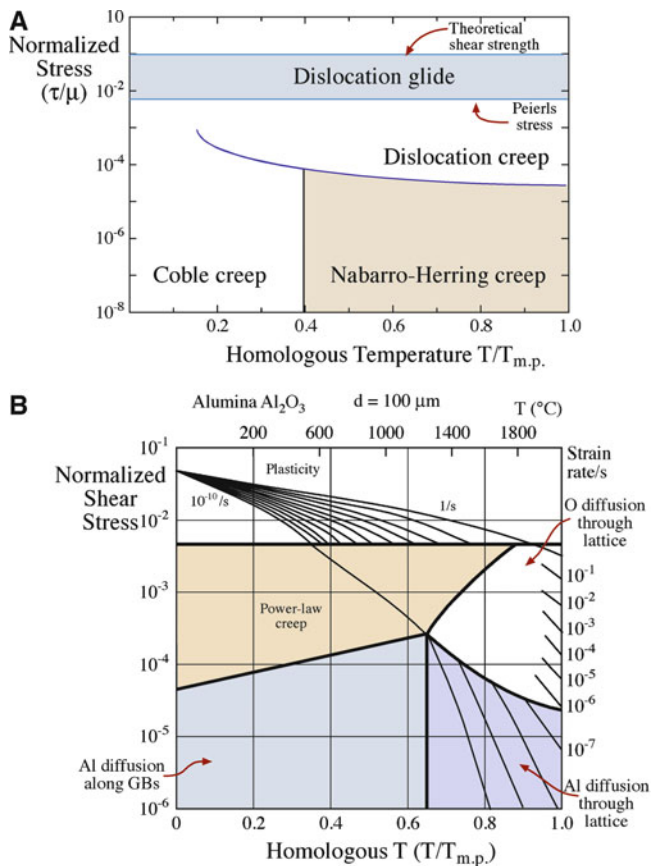


FIGURE 17.19. (A) Creep deformation map for a polycrystalline ceramic. (B) Creep deformation map for Al_2O_3 .

For a given ceramic, a specific creep mechanism may dominate at certain temperatures and stresses. This can be represented on a creep deformation map, as illustrated in Figure 17.19A for the general case and in Figure 17.19B for the specific case of Al_2O_3 . As you can imagine, these maps are based on a large amount of experimental data.

17.13 VISCOUS FLOW

Viscous flow is an important mechanism for permanent deformation in glasses. It allows us to form complex shapes, as shown in Figure 17.20. Viscous flow is also a mechanism by which ceramics containing IGFs undergo creep. Thus, it is a characteristic that is both beneficial and deleterious—but unavoidable at high temperature.

Under most conditions, oxide glasses behave as Newtonian fluids (i.e., the strain rate, $d\gamma/dt$, is a linear



FIGURE 17.20. Detail from a glass sculpture by Dale Chihuly.

function of applied shear stress, τ). An important consequence of this behavior is that when we draw glasses, such as during the formation of optical fibers, the cross section reduces at a constant rate. In other words, we don't get necking of narrow sections of the fiber. At high stress levels, non-Newtonian behavior, which is common in polymers, may be observed in oxide glasses.

Models of viscous flow

Absolute-rate theory: viscous flow is a thermally activated process involving a high-energy activated state. Viscosity follows an Arrhenius expression with activation energy for viscous flow, E_v . The preexponential term has a weaker dependence on temperature than the exponential term. This theory is applicable only over a narrow range of temperatures.

Free-volume theory: molecular motion involves the availability of vacancies. The vacancy volume is the free volume, V_F , of the liquid—approximately the difference in the volume of the liquid, V_L , and crystalline, V_C , forms. V_F is a function of temperature. D is a constant close to unity. The Williams-Landel-Ferry (WLF) equation uses a similar approach, where f_g is the fraction of the free volume at T_g , about 0.025, and β_L and β_C are the volumetric thermal expansion coefficients of the liquid and solid, respectively.

Excess-entropy theory: there is a decrease in the configurational entropy, S_c , of a liquid when it is cooled down—fewer molecular arrangements are possible.

This makes deformation more difficult. E_s is proportional to the potential energy barrier for molecular rearrangement.

VISCOUS FLOW

Newton's Law

$$\tau = \eta d\gamma/dt$$

EQUATIONS FOR VISCOUS FLOW

Arrhenius:

$$\eta = \eta_0 \exp\left(\frac{E_v}{RT}\right)$$

Turnbull and Cohen:

$$\eta = \eta_0 \exp\left(\frac{DV_c}{V_F}\right)$$

Williams-Landel-Ferry (WLF):

$$\eta = \eta_0 \exp\left(\frac{D}{f_g + (\beta_L - \beta_C)(T - T_g)}\right)$$

Adams-Gibbs:

$$\eta = \eta_0 \exp\left(\frac{E_s}{TS_c}\right)$$

Vogel-Fulcher-Tammann (VFT):

$$\eta = \eta_0 \exp\left(\frac{C}{T - T_0}\right)$$

The Vogel-Fulcher-Tammann (VFT) equation is an empirical expression relating η to T and can be interpreted in terms of the different models. The VFT expression is accurate over a wide range of temperatures and is widely used in many practical applications.

The viscosity of a specific glass depends on temperature, as shown in Figure 17.21. Glass blowing is often performed at viscosities of ~ 10 MPa·s. This is at the top end of the working range, which extends from 1 kPa·s

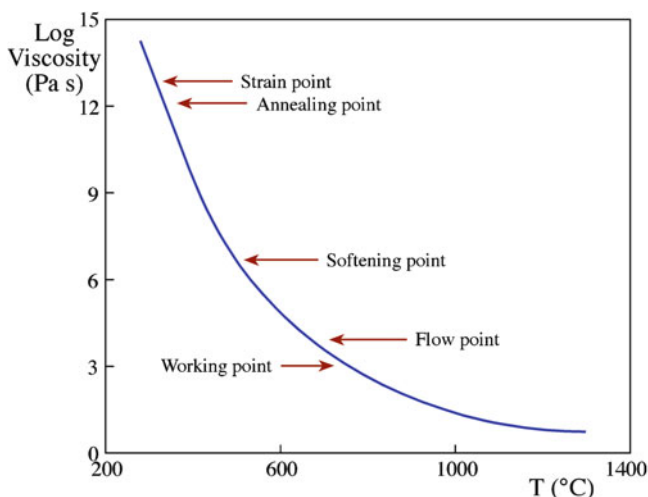


FIGURE 17.21. Temperature dependence of viscosity for a soda-lime-silica glass.



FIGURE 17.22. Microblown silica shape formed on oxidized SiC.

to 10 MPa·s. Figure 17.22 shows a microblown feature formed in a silica scale on oxidized SiC at $1,800^\circ\text{C}$, which for pure silica corresponds to the softening point. If the viscosity was at the fining temperature (~ 5 Pa·s), the gas would have been able to escape easily. If the viscosity were too high, the glass would not have been able to deform in this way.

There is also time dependence to the viscosity, particularly near T_g and above. At these temperatures, structural relaxation occurs.

17.14 SUPERPLASTICITY

Superplasticity is the ability of a material to sustain very large strains. From our discussions so far on the mechanical properties of ceramics, you may think it unlikely that any ceramic would exhibit superplasticity. Superplasticity, though has been observed in, for example, tetragonal ZrO_2 stabilized with Y_2O_3 . Elongations of 800% were observed for ceramics stabilized with 3 mol% Y_2O_3 and 1,038% for tetragonal zirconia stabilized with 2.5 mol% Y_2O_3 containing 5 wt% SiO_2 . The general requirements are that the grains should be:

- Small (typically $< 1 \mu\text{m}$)
- Equiaxed

The mechanism for superplasticity in ceramics must clearly be different from that in metal alloys because there

is no appreciable change in grain shape. Several models have been proposed. The one illustrated in Figure 17.23 involves grain switching and accounts for the constancy of grain shape during deformation, but it cannot account for the increase in surface area resulting from plastic deformation. Other models involve grain boundary sliding but, again, don't appear to fully account for the process.

Although superplasticity is a useful forming process for metals, it tends not to work for ceramics because of the problem of cavitation and the requirement of high temperatures.

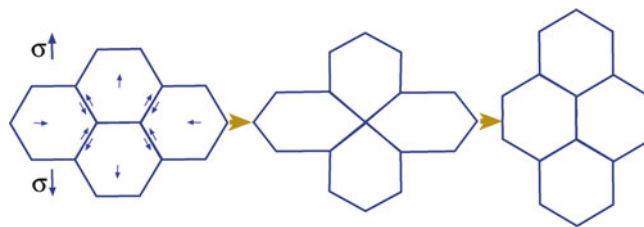


FIGURE 17.23. Model shows how grain switching can produce a shape change.

CHAPTER SUMMARY

Although we often think of the mechanical properties of ceramics entirely in terms of their brittleness, in this chapter we showed that plastic deformation is also important. The main difference between plasticity in ceramics and in metals is that for ceramics the primary mechanism of plastic deformation may not be the motion of dislocations. If dislocations are involved, then we are invariably at high temperatures. Plastic deformation is a key engineering design consideration in the use of ceramics in structural applications. Consequently, understanding creep behavior is essential, which means we have to understand point defects (see Chapter 11) and in many cases the role of IGFs (see Chapter 15). As an illustration of why we devoted an entire chapter to this topic, remember the example from the final section: elongations in excess of 1,000% have been observed in some ceramics. This is clearly not the conventional wisdom when it comes to ceramics and probably something that you would not have expected prior to reading this chapter. Unfortunately, we have not been able to come up with a clear explanation for this property.

PEOPLE AND HISTORY

Herring, W. Conyers (1914–2009) was Emeritus Professor of Applied Physics at Stanford University. He was elected to the National Academy of Sciences in 1968. In 1988, he could be seen in the café at Xerox PARC.

Nabarro, Frank Reginald Nunes (1916–2006). Born in London in 1916, he studied at Oxford and Bristol University. In 1953 he became head of the Physics Department at the University of the Witwatersrand in South Africa. He is remembered by name in Nabarro-Herring creep and the Peierls-Nabarro force.

von Mises, Richard (1883–1953). He was born in Lemberg, Austria-Hungary, which is now Lviv, Ukraine. A mathematician and engineer, he worked in a number of areas including statistics, probability theory, and mechanics. He died in Boston.

EXERCISES

- 17.1 An MgO single crystal is loaded in uniaxial compression, with the [001] direction parallel to the compression axis. Assuming that dislocation motion occurs on the primary slip system when the applied stress is 30 MPa, what is the inherent lattice resistance to dislocation motion?
- 17.2 The lattice parameter of MgO is $a = 0.4211$ nm. Calculate the distance between Mg^{2+} and O^{2-} ions prior to slip (Figure 17.5A, C) and at the midpoint position (Figure 17.5B, D) during slip on {100} and {110} planes
- 17.3 Figure 17.14 shows the hardening effect of NiO additions to MgO. Based on what you know about these two ceramics, would you expect the NiO/MgO system to show a complete range of solid solubility? You must justify how you arrived at your answer.
- 17.4 Figure 17.22 shows a microblown silica shape formed on SiC. What gas do you think would be formed at the SiO_2/SiC interface and lead to the shape shown? Would the gas be different at different temperatures?
- 17.5 For each of the ceramics listed in Table 17.1, would a tensile stress applied parallel to the c axis give a nonzero resolved shear stress?
- 17.6 The following dislocation reaction has been proposed for dislocation motion in graphite: $a/3 [2\bar{1}\bar{1}0] = a/3 [1\bar{1}00] + a/3 [10\bar{1}0]$ Is the reaction favorable as written? Justify your answer and state any assumptions that you make.

- 17.7 The addition of impurity atoms can pin dislocations in single crystals. The addition of small amounts (0.002%) of NdF_3 to CaF_2 can be very effective at increasing the yield stress because of the formation of point defect complexes. Using the Kröger–Vink notation, show that adding NdF_3 to CaF_2 can result in the formation of a defect complex.
- 17.8 Creep is a concern for structural ceramics at high temperatures. Discuss possible creep mechanisms for SiC and Si_3N_4 .
- 17.9 A major multinational company hires you as a consultant because of your knowledge of ceramics. You are asked to recommend a ceramic that has the maximum possible creep resistance at an operating temperature of $1,200^\circ\text{C}$. What material would you select and why? Also consider how you would process it.
- 17.10 Using the data in Figure 17.21, determine the activation energy for viscous flow in the soda-lime-silica glass. Based on your knowledge of glass structures, would you expect the activation energy to be higher or lower for a pure silica glass? Briefly justify your answer.
- 17.11 Which is softer— MgO or KCl ? What are the main deciding factors?
- 17.12 What can you learn from Figure 17.2?
- 17.13 Is Figure 17.3 consistent with Figure 17.4A?
- 17.14 Several secondary slip systems are missing from Table 17.1. Why are they missing, and what might they be?
- 17.15 Consider Table 17.2: what are the slip systems, and which obvious one is missing?
- 17.16 Derive equation 17.2.
- 17.17 Explain in words how MgO is deforming in each situation shown in Figure 17.8.
- 17.18 Explain the number of independent slip systems in Table 17.4.
- 17.19 When a dislocation moves from grain A to grain B in Figure 17.9, what happens to the grain boundary?
- 17.20 Are the two diagrams in Figure 17.13 consistent? Explain your reasoning.

REFERENCES

See also the references in Chapter 16.

GENERAL REFERENCES

- Cannon WR, Langdon TG (1983) Creep of ceramics: part 1. *J Mater Sci* 18:1–80
- Cannon WR, Langdon TG (1988) Part 2. *J Mater Sci* 23: 1–20
- Chan KS, Page RA (1993) Creep damage development in structural ceramics. *J Am Ceram Soc* 76:803–826, A review of creep behavior
- Cook RF, Pharr GM et al (1994) Mechanical properties of ceramics. In: *Materials science and technology*, vol 11. VCH, Germany, pp 339–407
- Davidge RW (1979) *Mechanical behaviour of ceramics*. Cambridge University Press, New York
- Green DJ (1998) *An introduction to the mechanical properties of ceramics*. Cambridge University Press, Cambridge, UK
- Nieh TG, Wadsworth J (1990) Superplastic ceramics. *Ann Rev Mater Sci* 20:117–140
- Poirier J-P (1985) *Creep of crystals: high-temperature deformation processes in metals, ceramics and minerals*. Cambridge University Press, Cambridge, UK
- Sprackling MT (1976) *The plastic deformation of simple ionic crystals*. Academic, London

SPECIFIC REFERENCES

- Buerger MJ (1930) Translation-gliding in crystals of the NaCl structural type. *Am Mineral* 15:174–187, and 226–238. The crystallographer not the \mathbf{b} vector. Before dislocations were widely appreciated
- Coble RL (1963) A model for boundary diffusion controlled creep in polycrystalline materials. *J Appl Phys* 34:1679–1682
- Gilman JJ (1959) Plastic anisotropy of LiF and other rocksalt-type crystals. *Acta Metall* 7:608–613
- Hall EO (1951) The deformation and aging of mild steel: III discussion of results. *Proc Phys Soc B64*:747–753
- Herring C (1950) Diffusional viscosity of a polycrystalline solid. *J Appl Phys* 21:437–445
- Nabarro FRN (1948) Report of a conference on strength of solids, The Physical Society, London, pp 75–90. The conference was held at Bristol University in the UK in 1947
- Petch NJ (1953) The cleavage strength of polycrystals. *J Iron Steel Inst (Lond)* 173:25
- Reusch E (1867) Ueber eine besondere Gattung von Durchgängen im Steinsalz und Kalkspath. *Ann Phys Chem* 132:443–444, and 449–450